

## A NEW $C^1$ FINITE ELEMENT: FULL HEPTIC

J. M. BOISSERIE

*Direction des Etudes et Recherches, Electricite de France, Chatou 78400, France*

### SUMMARY

A new  $C^1$  finite element complete in 7th degree polynomial basis is described and compared with other  $C^1$  elements in an eigen-elements analysis.

### INTRODUCTION

Among the many advantages of finite element methods special attention must be paid to the choice of many types of local approximations. In fact, we can keep constant the number of triangles while increasing the order of approximations. This point is central in adaptive systems like those proposed by Babuska<sup>1</sup> capable of improving accuracy in the vicinity of singularities.

What real gains do we obtain in increasing the degree of approximation? Houstis and Rice<sup>2</sup> have reported on an experimental study of the effectiveness of high order numerical methods applied to elliptic partial differential equations whose solutions have singularities. Their conclusion, in the case of rectangular domains, is: higher order is better.

Another advantage of finite element methods is their ability to incorporate—for certain orders of polynomial approximation—a required continuity of partial derivatives of unknown functions through the common boundary of two elements. This property has to be imposed when second derivatives appear in the expression of functionals associated with the partial differential equation. In mechanical problems this is the case for plates and shells. Then local rotations are given by expressions including first partial derivatives of displacement vector components, and continuity of these quantities is required. The classical expression to designate this type of element has been given by Fix and Strang:<sup>3</sup>  $C^1$  elements.

Using, like Caramanlian<sup>4</sup> and Mansfield,<sup>5</sup> rational functions, construction of  $C^1$  finite elements is possible. But we prefer keeping complete polynomial approximations like Ciarlet<sup>6</sup> and Zenisek.<sup>7</sup> This last author has given a remarkable theorem, for which we give the expression in two-dimensional space only. To achieve piecewise polynomial approximations of class  $C^q$ , the nodal parameters—at the vertices—must include *all derivatives of order less than or equal to  $2q$* . The polynomial must have at least degree  $4q + 1$ . To our knowledge, only the  $C^1$  full pentic due to Argyris *et al.*<sup>8</sup> satisfies all these conditions.

Another way to build  $C^1$  finite elements is known: to assemble a macro-element with three subtriangles, keeping in mind that  $C^1$  conditions must remain untouched. Historically we owe to Clough, Hsieh and Tocher<sup>9</sup> the first implementation of this type of element with a polynomial of third degree. Bernadou and Hassan<sup>10</sup> and the author of this note have implemented these elements. Recently, Torres *et al.*<sup>11</sup> have extended this method with polynomials of fifth degree.

In this paper, we present a  $C^1$  finite element complete in polynomial basis of 7th degree following Zenisek,<sup>7</sup> Ciarlet<sup>6</sup> and Bernadou and Boissarie.<sup>12</sup> This tentative approach may be compared with that of Tewarson<sup>13</sup> for ordinary differential equations and Jirousek<sup>14</sup> for plate problems.

### DEFINITIONS

The full heptic  $C^1$  triangular finite element, presented Figure 1, has 15 nodes:

- (i) three vertices  $a_1, a_2, a_3$ ;
- (ii) nine points:  $b_1, b_2, b_3, d_1, d_2, d_3, d_4, d_5, d_6$ ;
- (iii) three interior points  $e_1, e_2, e_3$ .

Among the nine edge points, six—the nodes  $d_i$ —have two degrees of freedom (d.o.f.'s):

- (i) the unknown function;
- (ii) the derivative of the unknown function counted normally to the edge.

On the edge, the three other points—the nodes  $b_i$ —have only one d.o.f: the derivative of the unknown function counted normally to the edge. The three interior points—the nodes  $e_i$ —have only one d.o.f: the unknown function. Zenisek proposes in his paper<sup>7</sup> a single point  $e_1$  with three degrees of freedom: the value of the function and two components of the gradient. We found this last solution more complicated for mesh elaboration. Finally the vertices—the nodes  $a_i$ —have, like P5, six d.o.f.'s: the function, two components of the gradient and three components of the second derivatives.

Why is this element  $C^1$  continuous?

Firstly we remark that on every edge 8 coefficients are given to determine the function: 2 times 3 at the vertices and 2 on the edge.

Secondly we verify that on every edge 7 coefficients are given to determine the gradient counted normally to the edge: 2 times 2 at the vertices and 3 on the edge.

All these coefficients are shared by two adjacent elements, and because we use a heptic basis, the required  $C^0$  and  $C^1$  properties are guaranteed.

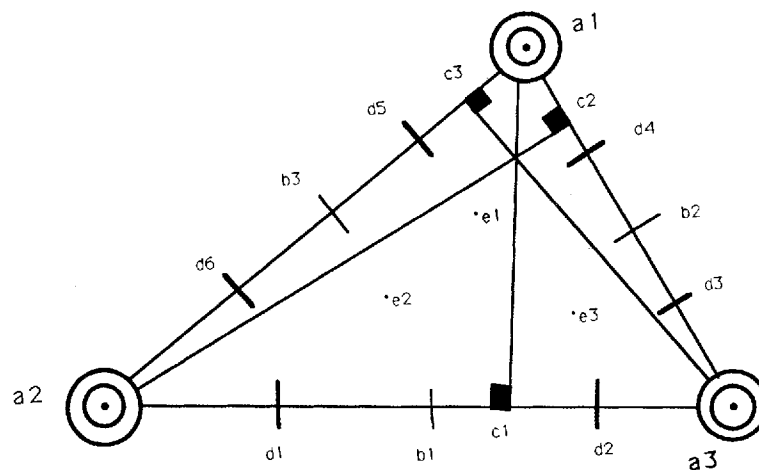


Figure 1

Following Bernadou and Boisserie,<sup>12</sup> shape functions may be calculated using *area co-ordinates* and *eccentricity parameters*. The appearance of these last terms results from the fact that the affine mapping associated with area co-ordinates does not leave invariant derivatives counted normally to the edges.

Let us consider a non-degenerate triangle with vertices

$$a_1(x_1, y_1), a_2(x_2, y_2), a_3(x_3, y_3)$$

We have the expression for current point  $(x, y)$  co-ordinates:

$$\begin{aligned} x &= x_1 L_1 + x_2 L_2 + x_3 L_3 \\ y &= y_1 L_1 + y_2 L_2 + y_3 L_3 \end{aligned} \quad (1)$$

where the *area co-ordinates*  $L_1, L_2, L_3$  satisfy the relation

$$L_1 + L_2 + L_3 = 1 \quad (2)$$

In the following, indices  $i+1, i+2, j+1, j+2$  take the values 1, 2, 3 modulo 3. Eccentricity parameters  $\eta_i$  are defined by the relation

$$\eta_i = [l_{i+2} - l_{i+1}] [l_{i+2} + l_{i+1}] / l_i^2 \quad (3)$$

with  $l_i^2 = (x_{i+2} - x_{i+1})^2 + (y_{i+2} - y_{i+1})^2$  and  $l_i$  the length of the side opposed to vertex  $i$ .

We have to calculate the first and second partial derivatives of unknown functions or, equivalently, to apply linear operators to the polynomial interpolator. We have the definition of these operators:

$$l_i \partial / \partial s_i = \partial / \partial L_{i+2} - \partial / \partial L_{i+1} \quad (4)$$

$$l_i l_j \partial^2 / \partial s_i \partial s_j = [\partial / \partial L_{i+2} - \partial / \partial L_{i+1}] [\partial / \partial L_{j+2} - \partial / \partial L_{j+1}] \quad (4a)$$

with  $\partial / \partial s_i$  the first partial derivative of a function of  $L_1, L_2, L_3$  counted along the side of length  $l_i$  opposed to vertices  $i$  and  $\partial^2 / \partial s_i \partial s_j$  the second partial derivative of a function of  $L_1, L_2, L_3$  taken successively along sides of length  $l_i$  and  $l_j$ .

Similarly, we have the expression for the first partial derivatives counted normally to an edge:

$$|a_i c_i| \partial / \partial n_i = -\partial / \partial L_i + [(1 + \eta_i) \partial / \partial L_{i+2} - (1 - \eta_i) \partial / \partial L_{i+1}] \quad (5)$$

with  $|a_i c_i|$  the length of vector  $a_i c_i$ , as shown on Figure 1.

Following Bernadou and Boisserie,<sup>12</sup> we establish a distinction between *local degrees of freedom* stemming from calculations in *area co-ordinates* and *global degrees of freedom* expressed in *Cartesian co-ordinates*, which are necessary to assemble elementary matrices and second members.

When we build an elementary stiffness matrix, we proceed in two steps. Firstly we use shape functions—basis functions—and numerical integration to obtain an expression for this matrix and its associated second member. We will comment on this point. Secondly we transform these entities from *local degrees of freedom* to *global degrees of freedom*.

Corresponding formulae are given in Bernadou and Boisserie<sup>12</sup> and will not be commented on here because the nature of the d.o.f.'s is identical to that of a P5 element.

## SHAPE FUNCTIONS

Relations (4), (4a) and (5) allow us to define a correspondence between degrees of freedom, nodes—following Figure 2—and elementary monomial components of complete heptic polynomial basis. We define:

## DEGREES OF FREEDOM NUMBERING

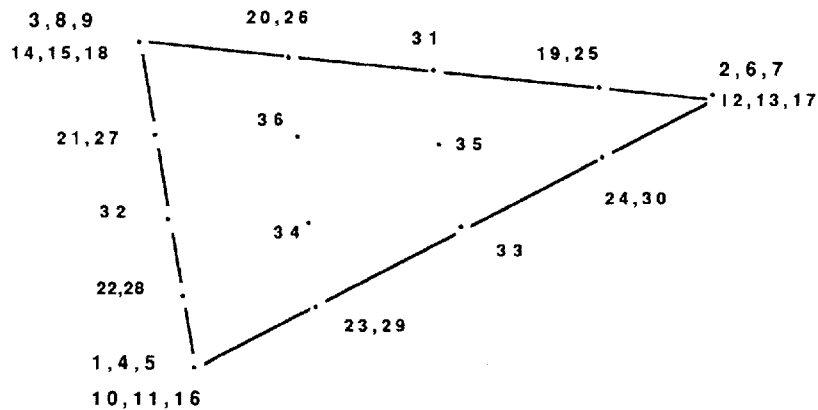


Figure 2

[P7]: the ordered set—following Table I—of 36 elementary homogeneous monomials of the heptic basis;

[DLLC]: the ordered set of 36 degrees of freedom;

[A]: the matrix of shape function coefficients.

The definition of the shape functions—degrees of freedom given as a function of elementary monomials—is equivalent to the relation

$$[\text{DLLC}] = [A] \cdot [\text{P7}] \quad (6)$$

$(36 \times 1) \quad (36 \times 36) \quad (36 \times 1)$

In the classical P5 case  $A$  is strictly upper-diagonal, as we can see in Reference 12, p. 71. In the P7 case the non-zero terms are below the diagonal. In  $A$  we count 360 non-zero elements, of which 166— $B_i$ —are distinct. Thirty-one  $B_i$  coefficients are constants and 135 depend on the *eccentricity coefficients*  $\eta_i$ . They are shown in Table II and ordered with these conventions:

- (i) at the beginning, we place  $B_i$  depending upon  $\eta_i$  and  $\eta_{i+1}$ —9 terms;
- (ii) then we place  $B_i$  depending linearly upon  $\eta_i$  and ordered by taking the values of  $\eta_i$  coefficients in increasing order—126 terms described by 42 expressions,
- (iii) then we have constants in increasing order—31 terms.

Finally 360 terms are presented in 82 lines.

In Reference 15 we can see how to place  $B_i$  and, for instance, perceive a simple property of the  $A$  matrix:

$$A_{ii} = 1 \quad \text{iff} \quad 1 \leq i \leq 9 \quad (7)$$

We have a similar property for P5  $C^1$  finite elements (Reference 12, p. 71).

## NUMERICAL INTEGRATION

The degree of numerical integration must match the degree of the shape functions. With numerical analysis techniques like the ones shown in Reference 12, it would be possible to show that in the

Table I. Table of monomials of area coordinates  $L_1, L_2, L_3$ 

P7(1)	$L_1^{**7}$
P7(2)	$L_2^{**7}$
P7(3)	$L_3^{**7}$
P7(4)	$L_3*L_1^{**6}$
P7(5)	$L_2*L_1^{**6}$
P7(6)	$L_2^{**6}*L_1$
P7(7)	$L_3*L_2^{**6}$
P7(8)	$L_3^{**6}*L_2$
P7(9)	$L_3^{**6}*L_1$
P7(10)	$L_3^{**2}*L_1^{**5}$
P7(11)	$L_2^{**2}*L_1^{**5}$
P7(12)	$L_2^{**5}*L_1^{**2}$
P7(13)	$L_3^{**2}*L_2^{**5}$
P7(14)	$L_3^{**5}*L_2^{**2}$
P7(15)	$L_3^{**5}*L_1^{**2}$
P7(16)	$L_3*L_2*L_1^{**5}$
P7(17)	$L_3*L_2^{**5}*L_1$
P7(18)	$L_3^{**5}*L_2*L_1$
P7(19)	$L_3^{**4}*L_2^{**3}$
P7(20)	$L_3^{**3}*L_2^{**4}$
P7(21)	$L_3^{**3}*L_1^{**4}$
P7(22)	$L_3^{**4}*L_1^{**3}$
P7(23)	$L_2^{**4}*L_1^{**3}$
P7(24)	$L_2^{**3}*L_1^{**4}$
P7(25)	$L_3^{**4}*L_2^{**2}*L_1$
P7(26)	$L_3^{**2}*L_2^{**4}*L_1$
P7(27)	$L_3^{**2}*L_2*L_1^{**4}$
P7(28)	$L_3^{**4}*L_2*L_1^{**2}$
P7(29)	$L_3*L_2^{**4}*L_1^{**2}$
P7(30)	$L_3*L_2^{**2}*L_1^{**4}$
P7(31)	$L_3^{**3}*L_2^{**3}*L_1$
P7(32)	$L_3^{**3}*L_2*L_1^{**3}$
P7(33)	$L_3*L_2^{**3}*L_1^{**3}$
P7(34)	$L_3^{**2}*L_2^{**2}*L_1^{**3}$
P7(35)	$L_3^{**2}*L_2^{**3}*L_1^{**2}$
P7(36)	$L_3^{**3}*L_2^{**2}*L_1^{**2}$

Table II.  $B(i)$  coefficients:  $0 < i < 167, 0 < k < 4$ 

$$\begin{aligned}
B(1) &= (-8002*ETA2 + 1621*ETA1 - 9321)/27 \\
B(2) &= (-1621*ETA2 + 8002*ETA1 - 9321)/27 \\
B(3) &= (2*(5215*ETA2 - 5215*ETA1 + 22396))/27 \\
B(4) &= (2*(5215*ETA3 - 5215*ETA2 + 22396))/27 \\
B(5) &= (-8002*ETA3 + 1621*ETA2 - 9321)/27 \\
B(6) &= (-1621*ETA3 + 8002*ETA2 - 9321)/27 \\
B(7) &= (8002*ETA3 - 1621*ETA1 - 9321)/27 \\
B(8) &= (2*(-5215*ETA3 + 5215*ETA1 + 22396))/27 \\
B(9) &= (1621*ETA3 - 8002*ETA1 - 9321)/27 \\
B(K+9) &= (8192*(-2*ETA(K)+1))/27 \\
B(K+12) &= (2*(-6091*ETA(K)-3151))/27 \\
B(K+15) &= (512*(-19*ETA(K)+13))/27
\end{aligned}$$

Table II (Contd.)

---

$B(K+18) = (1024 * (-ETA(K) + 1)) / 3$		
$B(K+21) = (512 * (-17 * ETA(K) - 91)) / 27$		
$B(K+24) = (-2783 * ETA(K) - 1838) / 9$		
$B(K+27) = (-1024 * (ETA(K) + 1)) / 9$		
$B(K+30) = (245 * (-ETA(K) + 1)) / 3$		
$B(K+33) = (-513 * ETA(K) - 571) / 9$		
$B(K+36) = (5 * (-31 * ETA(K) + 85)) / 3$		
$B(K+39) = (-375 * ETA(K) - 28) / 9$		
$B(K+42) = (-719 * ETA(K) - 179) / 18$		
$B(K+45) = (512 * (-ETA(K) + 31)) / 27$		
$B(K+48) = (-53 * ETA(K) + 115) / 6$		
$B(K+51) = (-127 * ETA(K) - 1051) / 18$		
$B(K+54) = (-13 * ETA(K) - 14) / 6$		
$B(K+57) = (-13 * ETA(K) + 44) / 6$		
$B(K+60) = (-11 * ETA(K) - 2) / 6$		
$B(K+63) = (-19 * ETA(K) - 15) / 12$		
$B(K+66) = (-ETA(K) + 3) / 4$		
$B(K+69) = (-3 * ETA(K) - 35) / 12$		
$B(K+72) = (ETA(K) + 3) / 4$		
$B(K+75) = (3 * ETA(K) - 35) / 12$		
$B(K+78) = (19 * ETA(K) - 15) / 12$		
$B(K+81) = (11 * ETA(K) - 2) / 6$		
$B(K+84) = (13 * ETA(K) - 14) / 6$		
$B(K+87) = (13 * ETA(K) + 44) / 6$		
$B(K+90) = (127 * ETA(K) - 1051) / 18$		
$B(K+93) = (53 * ETA(K) + 115) / 6$		
$B(K+96) = (512 * (ETA(K) + 31)) / 27$		
$B(K+99) = (719 * ETA(K) - 179) / 18$		
$B(K+102) = (375 * ETA(K) - 28) / 9$		
$B(K+105) = (5 * (31 * ETA(K) + 85)) / 3$		
$B(K+108) = (513 * ETA(K) - 571) / 9$		
$B(K+111) = (245 * (ETA(K) + 1)) / 3$		
$B(K+114) = (1024 * (ETA(K) - 1)) / 9$		
$B(K+117) = (2783 * ETA(K) - 1838) / 9$		
$B(K+120) = (512 * (17 * ETA(K) - 91)) / 27$		
$B(K+123) = (1024 * (ETA(K) + 1)) / 3$		
$B(K+126) = (512 * (19 * ETA(K) + 13)) / 27$		
$B(K+129) = (2 * (6091 * ETA(K) - 3151)) / 27$		
$B(K+132) = (8192 * (2 * ETA(K) + 1)) / 27$		
$B(136) = (-1024)$	$B(146) = (-13) / 6$	$B(157) = 21$
$B(137) = (-4621) / 27$	$B(147) = (-5) / 3$	$B(158) = 256 / 9$
$B(138) = (-1024) / 9$	$B(148) = (-1) / 2$	$B(159) = 42$
$B(139) = (-2048) / 27$	$B(149) = 1 / 2$	$B(160) = 394 / 9$
$B(140) = (-48)$	$B(150) = 1$	$B(161) = 490 / 9$
$B(141) = (-364) / 9$	$B(151) = 3 / 2$	$B(162) = 512 / 9$
$B(142) = (-32)$	$B(152) = 13 / 6$	$B(163) = 256 / 3$
$B(143) = (-271) / 9$	$B(153) = 6$	$B(164) = 160$
$B(144) = (-31) / 3$	$B(154) = 7$	$B(165) = 2048 / 9$
$B(145) = (-13) / 3$	$B(155) = 28 / 3$	$B(166) = 3072$
	$B(156) = 16$	

---

Table III

Type of element	Number of Gauss points	Relative time of calculation
P5	12	0.61
P5	16	0.78
P7	25	2.21

case of P7 elements and in a Kirchhoff plate context, integration schemes must be exact for polynomials up to degree 10 for stiffness matrices and up to degree 12 for mass matrices. This last fact is a consequence of the existence of first degree differential terms in mass matrices.<sup>16</sup>

Dunavant<sup>17</sup> has given exact Gaussian numerical integration schemes, exact for polynomials up to the 20th degree. In the following examples—plate dynamical analysis—we take, following the notations of this last author,  $ng = 25$  for a stiffness matrix and  $ng = 37$  for a mass matrix satisfying the preceding conditions. P7 elements may be used in a context of shell analysis following Koiter's equations, as in Reference 16. Then we choose integration schemes corresponding to  $ng = 33$  for stiffness matrices and  $ng = 42$  for mass matrices.

If we take as a basic unit the time necessary to calculate a plate finite element of reduced Hsieh Clough Tocher type with 9 integration points, we have for corresponding P5 and P7 elements the results given in Table III.

For a certain part that is a consequence of a better implementation of P5 and P7 elements, Gaussian points co-ordinates are known and corresponding values of monomials are calculated only as an initial process.

### NUMERICAL EXPERIMENTS

Because we are aiming at verifying a finite element, and not a complete physical situation with a complicated energy density, we take as an example the determination of modal frequencies and mode shapes of a thin rhombic plate with an angle  $\phi = \pi/4$ .

The middle surface  $S$  of the plate is the image in  $\mathcal{R}^2$  of a bounded open set  $\Omega$  of  $\mathcal{R}^2$  with a  $\Gamma$  boundary through a mapping  $\Phi \in \mathcal{R}^2$ :

$$\begin{aligned}x^1 &= H_1 \xi_1 + H_2 \xi_2 \cos \phi \\x^2 &= H_2 \xi_2 \sin \phi \\H_1 &= H_2 = 10 \text{ m}\end{aligned}\tag{8}$$

The unknown function is the normal displacement to the middle surface  $S$ :  $u$ .

The open subset  $\Omega$  and its boundary  $\Gamma$  are defined by

$$0 < \xi_1 < 1 \quad 0 < \xi_2 < 1\tag{9}$$

Boundary conditions on  $\Gamma$  are

$$u = 0 \quad du/dn = 0, \quad \text{all edges clamped}\tag{10}$$

The following numerical values are taken: Young's modulus:  $200 \times 10^9 \text{ N/m}^2$ , Poisson's coefficient: 0.3, uniform thickness: 0.05 m.

Table IV. Thin rhombic plate ( $\pi/4$ ) frequencies in Hertz

	HCTR	HCTC	P5	P7
17	—	58·3372	—	57·8496
16	—	56·1840	—	55·8253
15	—	54·5022	—	53·3930
14	—	52·5856	52·1169	52·0936
13	—	47·6324	47·4307	47·4306
12	47·3017	45·5469	44·8860	44·8657
11	45·9309	44·5490	44·1815	44·1810
10	38·7119	37·4888	37·0920	37·0914
9	36·3959	35·5791	35·3997	35·4045
8	35·1859	34·7782	34·6748	34·6887
7	30·8865	30·1128	29·9027	29·9047
6	28·0876	27·6885	27·6268	27·6268
5	24·3127	23·7901	23·6888	23·6888
4	19·1089	18·9594	18·9299	18·9342
3	18·1867	17·8992	17·8556	17·8552
2	12·9632	12·8348	12·8216	12·8216
1	7·9527	7·9086	7·9035	7·9042

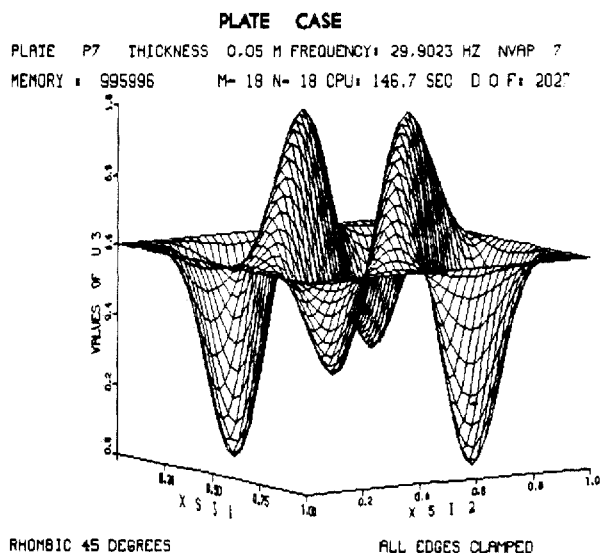


Figure 3

The mass matrices are fully consistent. Four  $C^1$  finite elements are taken into consideration while keeping constant the total number of nodes:

HCTR	Reduced Hsieh-Clough-Tocher	3 nodes $o(h)$
HCTC	Complete Hsieh-Clough-Tocher	6 nodes $o(h^2)$
P5	Full quintic Argyris	6 nodes $o(h^4)$
P7	Full heptic	15 nodes $o(h^6)$



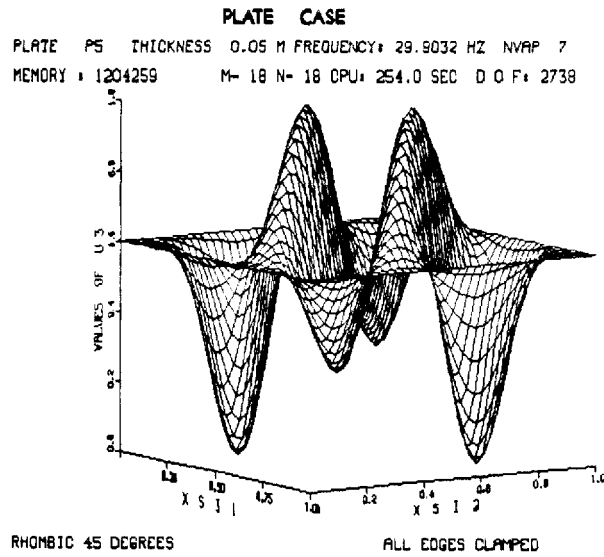


Figure 4

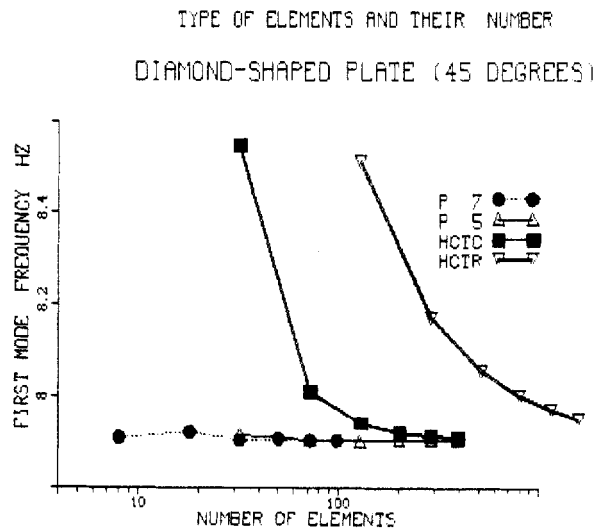


Figure 5

Here, we present two sets of results.

- (i) On Table IV we can read the frequencies obtained with all these  $C^1$  finite elements on a mesh of  $14 \times 14$  nodes. We can verify that purely polynomial elements are more precise. On Figures 3 and 4 we can see a representation of the 7th eigenshape—obtained with two different elements, P7 and P5 on a mesh of  $18 \times 18$  nodes—and evaluate qualitatively the cohesion of results.

TYPE OF ELEMENTS AND THEIR NUMBER  
DIAMOND-SHAPED PLATE (45 DEGREES)

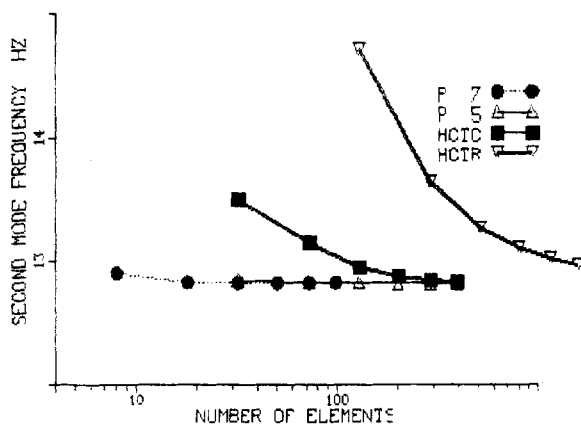


Figure 6

TYPE OF ELEMENTS AND THEIR NUMBER  
DIAMOND-SHAPED PLATE (45 DEGREES)

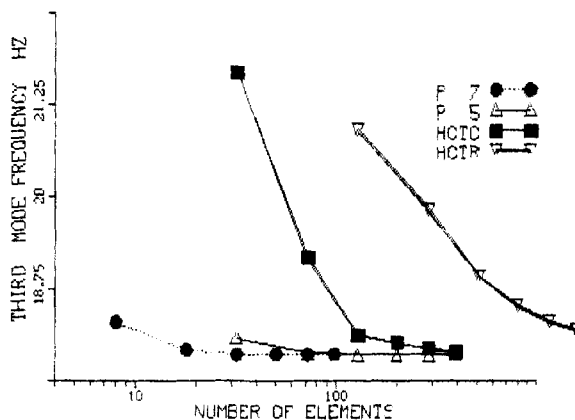


Figure 7

- (ii) On Figures 5, 6 and 7 we can follow the evolution of results for the three first frequencies through changing the number of elements.

All these results depend slightly on the spectral analysis software and its algorithms, which proceed iteratively.

### CONCLUSION

Generation of purely polynomial finite elements is more difficult in the  $C^1$  case than in the  $C^0$  case. This is due to the non-affine behaviour of normal derivatives to an edge and to the necessity of

having degrees of freedom of a *second derivative type*. This last fact has relatively less influence in the new element.

Meanwhile the results here presented corroborate with those of Bennighof and Meirovitch<sup>18</sup> showing better and more economic results obtained by increasing the degree of polynomial approximation for spectral analysis. In these situations, reduction of the number of d.o.f.'s is crucial and increases the economy of the process. Using successively P5 and P7 we have more confidence in the results obtained.

#### REFERENCES

1. I. Babuska, 'The  $p$  and  $h$ - $p$  of the finite versions of the finite element method. The state of the art', in R. Vough (ed.), *Finite Element Method Workshop*, Springer-Verlag, Berlin, 1987.
2. E. N. Houstis and J. R. Rice, 'High order methods for elliptic partial differential equations with singularities', *Int. j. numer. methods eng.*, **18**, 737–754 (1982).
3. G. J. Fix and G. Strang, *An Analysis of the Finite Element Method*, Prentice-Hall, Englewood Cliffs, N.J., 1973.
4. C. Caramanlian, 'A solution to the  $C^1$  continuity problem in plate bending', *Int. j. numer. methods eng.*, **19**, 1291–1317 (1983).
5. L. Mansfield, 'Higher order compatible triangular finite elements', *Numer. Mathematik*, **22**, 89–97 (1974).
6. P. G. Ciarlet, *The Finite Element Method for Elliptic Problems*, North-Holland, Amsterdam, 1975.
7. A. Zenisek, 'Interpolation polynomials on the triangle', *Numer. Mathematik*, **15**, 283–296 (1970).
8. J. H. Argyris, I. Fried and D. W. Scharpf, 'The Tuba family of plate elements for the matrix displacement method', *Aeronaut. J. Roy. Aeronaut. Soc.*, **72**, 701–704 (1968).
9. R. W. Clough and J. L. Tocher, 'Finite element stiffness matrices for analysis of plates in bending', *Proc. Conf. on Matrix Methods in Structural Mechanics*, Wright Patterson Air Force Base, Ohio, 1965.
10. M. Bernadou and K. Hassan, 'Basic functions for general Hsieh-Clough-Tocher triangles completed or reduced', *Int. j. numer. methods eng.*, **17**, 784–789 (1981).
11. J. Torres, A. Samartin, V. Arroyo and J. Diaz del Valle, 'A  $C^1$  finite element family for Kirchhoff plate bending', *Int. j. numer. methods eng.*, **23**, 2005–2029 (1986).
12. M. Bernadou and J. M. Boissarie, *The Finite Element Method in Thin Shell Theory: Application to Arch Dam Simulations*, Birkhäuser, Boston, 1982.
13. R. P. Tewarson, 'A seventh order numerical method for solving boundary value non-linear differential equations', *Int. j. numer. methods eng.*, **18**, 1313–1319 (1982).
14. J. Jirousek, 'Hybrid-Trefftz plate bending elements with  $p$ -method capabilities', *Int. j. numer. methods eng.*, **24**, 1367–1393 (1987).
15. J. M. Boissarie, 'Quelques remarques sur les éléments finis  $C^1$  dans  $\mathcal{R}^{21}$ ', Internal Report, D.E.R E.D.F., 1988.
16. M. Bernadou and J. M. Boissarie, 'On the computation of stresses and free vibration modes in a general thin shell—Application to an arch dam', *Proceedings of the China-France Symposium on Finite Elements Methods*, Science Press, Beijing and Gordon and Breach, New York, 1983.
17. D. A. Dunavant, 'High degree efficient symmetrical Gaussian rules for the triangle', *Int. j. numer. methods eng.*, **21**, 1129–1148 (1985).
18. J. K. Bennighof and L. Meirovitch, 'Eigenvalue convergence in the finite element method', *Int. j. numer. methods eng.*, **23**, 2153–2165 (1986).